Diastereomer recognition of oxytetracycline and its 4-epimer by electrospray ionization mass spectrometry and mechanistic investigation

Dear Sir,

Tetracyclines (TCs) are a family of antibiotics used in human and veterinary medicine and as animal feed supplement. They are broad-spectrum agents, which show activities against a variety of Gram-positive and Gram-negative bacteria like chlamydia and rickettsia [1]. They are widely used because of the absence of major adverse side effects. The first generation of TCs includes chlortetracycline and oxytetracycline, which were discovered in the late 1940s from natural products. The second generation, such as tetracycline (also discovered from natural sources) and doxycycline (produced by semi-synthesis) came later [2]. However, because of their extensive usage, microbial resistance has emerged [3]. In order to overcome this problem, the third generation of TCs, also called glycylcycline, was discovered [4]. Tegecycline, the first glycylcycline, was first approved by the FDA in 2005 [5].

Structurally speaking, typical TC drugs have four six-membered rings, of which the D ring is aromatic (Figure 1A). In most TCs, the 4-epimers occur as impurities. Previous studies show that 4-epimerization is the favored degradation route for TCs. The 4-epimers could be formed during aqueous storage at mild acidic conditions (pH 2~6) [6,7]. Compared to the TCs, the 4-epimers only show a slight structural change,

with a flipped position of the dimethylamino group in C-4 position. However, the orientation of this group is very important since the relative activity of the 4-epimer is only 2 % of this of tetracycline along with a higher toxicity [2,8].

The study of isomers has always been an interesting issue in mass spectrometry (MS) [9]. Among them, epimers are particularly difficult to study, as they have exactly the same molecular mass and differ only in one asymmetric carbon. Recently, with the development of soft ionization technologies, MS has become a useful tool to investigate isomers, as it could differentiate between compounds with subtle differences [10-13]. Because of its usefulness, energy resolved mass spectrometry (ERMS) is frequently used to differentiate a series of diastereomers carrying functional groups like amines, carboxylic acids, alcohols or amino acids [12,14]. Theoretical calibration shows that the discrimination comes from the configuration difference, which results in deviating fragments in the mass spectra. Up until now, only one pair of tetracycline-like diastereomers was differentiated by MS [15]. However, the studied molecules did not have the same structure as TCs, since both the C and D rings were aromatic, which behave differently in the gas phase.

In the present work, oxytetracycline and its 4-epimer were successfully differentiated by the collision induced dissociation (CID) spectra of the protonated ions. The fragments acquired by ion trap MS were all explained and elemental compositions of the precursor and product ions were confirmed by electrospray ionization - quadrupole time-of-flight (ESI-QTOF) MS/MS. Furthermore, theoretical calibration was used to explain the fragmentation routes.

The ESI-MS^n analyses were carried out on a Bruker 3000^{plus} ion trap mass spectrometer (Bruker-Franzen Analytik GmbH, Bremen, Germany). An electrospray ionization (ESI) source sprayed the sample solution at a flow rate of 5 μL/min. Nitrogen was used as nebulizer and drying gas. Helium served as collision and damping gas in the ion trap. The optimized settings for the mass spectrometer in positive mode were as follows: nebulizer gas flow rate: 15 psi; drying gas flow rate: 5 L/min; spray voltage: 4.0 kV; ion source temperature: 250 °C; scan range: *m/z* 50-800. For MS/MS experiments, the collision energy was set between 0.18 and 0.45 V to perform ERMS.

Accurate MS experiments were carried out on an Agilent 6538 quadrupole time-of-flight (QTOF) mass spectrometer (Agilent, Singapore, Singapore), which was equipped with a dual-spray ESI source. Instrument control and data acquisition were performed with Mass Hunter B.06.01 software from Agilent. A mixture of ammonium trifluoroacetate, purine and hexakis (1H, 1H, 3H-tetrafluoropropoxy) phosphazene was used for internal calibration. The samples were infused into the source chamber by a Cole-Parmer syringe pump at a rate of 5 μL/min. The optimized settings for the mass spectrometer in positive mode were as follows: nebulizer gas flow rate: 15 psi; drying gas flow rate: 5 L/min; spray voltage: 4.0 kV; ion source temperature: 300 °C; scan range: *m/z* 50-1000. For MS/MS experiments, the collision energy was set between 5 and 10 V to maximize the ion current in the spectra.

Theoretical calculations were performed with the Gaussian 03 program (Revision C.02) (Gaussian, Wallingford, CT, USA) [16]. Structures of the key species were

optimized using the density functional theory (DFT) method at the B3LYP/6-31G(d) level. All reactants, intermediates and products were identified as true minima in energy by the absence of imaginary frequencies. Transitional states were identified by the presence of one single imaginary vibrational frequency and the normal vibrational mode, and further confirmed by intrinsic reaction coordinates (IRC) analysis. Vibrational frequencies and zero-point energies (ZPE) for all the critical species were calculated at the same level. DFT-optimized structures were shown by GaussView software (version 3.09) to yield higher-quality images of the determined structures. The energies discussed here are the sum of the electronic and thermal free energies.

Sample solutions of oxytetracycline and its 4-epimer were prepared in methanol - water (90:10, v/v) at a concentration of 10 μg/mL. They were injected directly into the ESI source and analyzed in the positive mode. The two compounds showed high abundant $[M+H]^+$ ions at *m/z* 461, both in ion trap MS and QTOF MS, allowing further CID analysis.

The CID spectrum of the protonated oxytetracycline acquired by ion trap MS is shown in Figure 2A. It is dominated by the ion at *m/z* 443, which is formed by the neutral loss of H_2O (18 Da) from the precursor ion. This fragment ion is characteristic for TCs with a tertiary hydroxyl group located at C-6. MS^3 experiments with ion trap MS on the protonated oxytetracycline showed that the other major peak at *m/z* 426 was formed by neutral loss of NH_3 (17 Da) from *m/z* 443 (Figure 2B). The fragment ion at *m/z* 443 could also lose dimethylamine (45 Da) to form the fragment ion at *m/z* 398, with further loss of NH_3 (17 Da) to form the fragment ion at *m/z* 381. The

fragment ion at *m/z* 426 could further lose H_2O (18 Da) to form the fragment ion at *m/z* 408 or dimethylamine (45 Da) to form the fragment ion at *m/z* 381. All these fragmentation routes are similar to those reported previously [17]. To confirm the proposed ions, QTOF MS/MS experiments were conducted. The exact mass data are shown in the Supplementary Material, with a maximum error of 5.5 ppm, indicating good mass accuracy.

Under the same conditions, the CID spectrum of the protonated 4-epimer (Figure 2C) was compared with oxytetracycline. Although the CID spectrum of 4-epioxytetracycline showed similar fragmentation routes compared to oxytetracycline, their fragmentation patterns were not identical. Indeed, compared to the CID spectrum of oxytetracycline, its 4-epimer showed an abundant fragment ion at *m/z* 444 with almost the same intensity as the fragment ion at *m/z* 443. The fragment ion at *m/z* 444 could be formed by neutral loss of NH_3 (17 Da), which was negligible in the spectrum of oxytetracycline. Moreover, the base peak was at *m/z* 426 instead of *m/z* 443. The fragment ion at *m/z* 426 was two times as intense as the fragment ion at *m/z* 443. In addition, the fragment ions at *m/z* 408 and *m/z* 398, which were observed for oxytetracycline, were not detected in the spectrum of its 4-epimer. MS^3 experiments with ion trap MS on the protonated 4-epimer showed that the fragment ion at *m/z* 426 could be formed through two routes: neutral loss of H_2O (18 Da) from *m/z* 444 (Figure 2D) or neutral loss of NH_3 (17 Da) from *m/z* 443 (Figure 2E). As reported previously, these are two parallel reaction routes [17]. For oxytetracycline, the fragmentation pathways were dominated by the reaction initiated

by the loss of water (18 Da), yielding a base peak at *m/z* 443. Since the two parallel fragmentation reactions showed similar abundance, the common further fragment ion at *m/z* 426 showed a higher abundance for the 4-epimer (Figure 2C). Although the two epimers only showed a configuration difference in one carbon atom, their protonated species apparently showed chiral recognition in the gas phase.

ERMS was recorded between 0.18 V and 0.42 V (Figure 3) for oxytetracycline and its 4-epimer. The base peak was changed from the protonated molecule to *m/z* 443 at 0.30 V for oxytetracycline. In contrast, it changed to *m/z* 426 at 0.33 V for the 4-epimer. At various collision energies, *m/z* 444 was negligible and *m/z* 443 was more abundant than *m/z* 426 for oxytetracycline. However, for the 4-epimer, *m/z* 443 showed similar abundance as *m/z* 444. Furthermore, *m/z* 443 was clearly less abundant than *m/z* 426.

Theoretical calculations were performed to examine the mechanistic difference in the CID-MS of the two isomers. Considering thermochemistry, the most plausible protonation site of oxytetracycline might be the dimethylamino group in C-4 position [17]. The fragmentation pathways of oxytetracycline and its 4-epimer are proposed in Scheme 1 to rationalize these observations. In path 1, the ionizing proton in the protonated molecule (0 kJ/mol) located at the dimethylamino group in C-4 position migrated to the hydroxyl group in C-6 position via transitional state TS-1 leading to **Ion a** at *m/z* 443. The activation barrier of the proton transfer process was 75.9 kJ/mol, which indicated that the proton transfer was the rate determining step to form **Ion a**. Further loss of NH_3 (17 Da) could result from two pathways. Path 1.1 was initiated by

the 1,2-H shift to form the intermediate **Int-1** (12.2 kJ/mol) through TS-2 (112.5 kJ/mol). With the double bond transfer, the proton of the hydroxyl group at the C-12 position was activated. This could further migrate to the carbonyl group at the C-1 position through TS-3 (30.1 kJ/mol) to form **Int-2** (12.2 kJ/mol). Subsequently, the proton could migrate to the amide group to form **Int-3** (85.7 kJ/mol) through TS-4 (86.7 kJ/mol). With neutral loss of NH_3 (17 Da), it could form **Ion b** (231.8 kJ/mol). The path is in accordance with the pathway proposed in literature [21]. As can be seen from the optimized configuration, the proton of the hydroxyl group at C-3 is close to the oxygen atom of the amide group (Figure 1B). In path 1.2, **Int-4** (141.5 kJ/mol) was formed through TS-5 (146.3 kJ/mol) via a direct six membered ring proton transfer. Further loss of NH_3 (17 Da) from **Int-4** could form **Ion c** (185.9 kJ/mol). The energy of the rate determining step for path 1.1 (TS-2, 112.5 kJ/mol) was lower than for path 1.2 (TS-5, 146.3 kJ/mol), which implied that path 1.1 was more accessible. Similar as path 1.2, the protonated molecular ion in path 2 could lose NH_3 (17 Da) through TS-6 (132.2 kJ/mol) and a six membered ring proton transfer to form intermediate **Int-5** (112.5 kJ/mol) prior to fragmentation. After bond breakage, it lost NH_3 (17 Da) to form **Ion d** (157.0 kJ/mol). Afterwards, it could further lose H_2O to form **Ion c** at *m/z* 426 (185.9 kJ/mol). As the proton in the molecule could migrate through many sites with relatively low energy barriers, it was also a good proof of the mobile proton model [18-20]. Comparing the energy barrier of path 1 with path 2, the rate determining step for path 1 is **TS-1** (75.9 kJ/mol), while for path 2 this is **TS-6** (132.2 kJ/mol). Thus, path 1 (loss of H_2O) is far more accessible than path 2 for

oxytetracycline, which is in accordance with the mass spectrum.

The optimized configuration of the protonated 4-epioxytetracycline is also shown in Figure 1B. The potential energy diagrams of oxytetracycline and its 4-epimer are shown in Figure 4. The 4-epioxytetracycline showed a similar fragmentation route as oxytetracycline, but the free energies were significantly different. For the optimized $[M+H]^+$, the protonated 4-epimer showed a higher energy (5.7 kJ/mol). In path 1, the protonated molecule lost H_2O through **TS-1′** (91.2 kJ/mol) to form **ion a′** (69.9 kJ/mol). In path 2, the loss of NH_3 was formed through intermediate **Int-5′** (104.4 kJ/mol) following **TS-6′** (116.4 kJ/mol). For oxytetracycline, the rate determining step for loss of NH_3 (**TS-6,** 132.2 kJ/mol) is about two times higher than the rate determining step for loss of H_2O (**TS-1,** 75.9 kJ/mol). Thus, the $[M+H-H_2O]^+$ ion at *m/z* 443 is the most abundant ion while the $[M+H-NH_3]^+$ ion at *m/z* 444 is negligible. However, for the 4-epimer, the free energy of the rate determining step for loss of NH_3 (**TS-6′,** 116.4 kJ/mol) is close to the loss of H_2O (**TS-1′,** 91.2 kJ/mol). As a result, the $[M+H-NH_3]^+$ ion at *m/z* 444 showed similar abundance as the $[M+H-H_2O]^+$ ion at *m/z* 443. Moreover, the lowest fragmentation determining step for oxytetracycline is **TS-1** (75.9 kJ/mol), which is lower than **TS-1′** (91.2 kJ/mol) for the 4-epimer. Thus, oxytetracycline had more tendency to form fragment ions, which is in correspondence with the ERMS result. In conclusion, the fragmentation behavior of this pair could be nicely rationalized based on differences in thermochemistry.

For oxytetracycline and its 4-epimer, the optimized conformation of the respective **Ion a**, **Ion b**, **Ion c** and **Ion d** are given in the Supplementary Material.

Summing up the above discussed results, protonated species of oxytetracycline and its 4-epimer were successfully differentiated by CID spectra in the positive mode. Elemental compositions of all ions were confirmed by high resolution MS. The CID spectrum of 4-epioxytetracycline showed an abundant fragment ion at *m/z* 444, which was as high as the fragment ion at *m/z* 443 and which was negligible in the spectrum of oxytetracycline. ERMS revealed that for oxytetracycline the base peak changed at 0.30 V and for its 4-epimers at 0.33 V. DFT calculations were employed to find the most reasonable fragmentation pathways, as well as the reason of their discrimination. The results showed that the fragmentation pathways were greatly influenced by the 3D configuration and by the energy barriers throughout the reaction process.

ACKNOWLEDGEMENT

The authors gratefully acknowledge the financial support from Zhejiang Provincial Public Welfare Technology Application and Research Project of China (LGF19H300001). Computer time was made available on the SGI Aktix 450 server at the Computational Center for Molecular Design of Organosilicon Compounds, Hangzhou Normal University

KEYWORDS

oxytetracycline, 4-epimer, differentiation, tandem mass spectrometry, density functional theory

AUTHORS

Peixi Zhu,[1,2] Kezhi Jiang,[3] Liya Hong,[4] Weike Su,[1] Ann Van Schepdael,[2] Erwin Adams[2]

[1] College of Pharmaceutical Sciences, Zhejiang University of Technology, Hangzhou 310014, Zhejiang, China

[2] KU Leuven, University of Leuven, Department of Pharmaceutical and Pharmacological Sciences, Pharmaceutical Analysis, Herestraat 49, O&N2, PB 923, 3000 Leuven, Belgium

[3] Key Laboratory of Organosilicon Chemistry and Material Technology, Hangzhou Normal University, Zhejiang, China

[4] Zhejiang Institute for Food and Drug Control, Hangzhou 310053, Zhejiang, China

Correspondence

Prof. Dr. Weike Su, College of Pharmaceutical Sciences, Zhejiang University of Technology, Hangzhou, China, 310014

E-mail address: pharmlab@zjut.edu.cn

REFERENCES

1. I. Chopra, M. Roberts. Tetracycline antibiotics: mode of action, applications, molecular biology, and epidemiology of bacterial resistance, *Microbiol. Mol. Biol. Rev.* **2001**, 65, 232.
2. J.R. Brown, D.S. Ireland. Structural requirements for tetracycline activity, *Adv. Pharmacol. Chemother.* **1978**, 15, 161.

3. Y. Zhang, J. Geng, H. Ma, H. Ren, K. Xu, L. Ding. Characterization of microbial community and antibiotic resistance genes in activated sludge under tetracycline and sulfamethoxazole selection pressure, *Sci. Total. Environ.* **2016**, 571, 479.
4. I. Chopra. Glycylcyclines: third-generation tetracycline antibiotics, *Curr. Opin. Pharmacol.* **2001**, 1, 464.
5. L.R. Peterson. A review of tigecycline- the first glycylcycline, *Int. J. Antimicrob. Ag.* **2008**, 32, S215.
6. G. Kahsay, J. Maxa, A. Van Schepdael, J. Hoogmartens, E. Adams. Development and validation of a reversed-phase liquid chromatographic method for analysis of demeclocycline and related impurities, *J. Sep. Sci.* **2012**, 35, 1310.
7. G. Kahsay, F. Shraim, P. Villatte, J. Rotger, C. Cassus-Coussère, A. Van Schepdael, J. Hoogmartens, E. Adams. Development and validation of a reversed phase liquid chromatographic method for analysis of oxytetracycline and related impurities, *J. Pharm. Biomed. Anal.* **2013**, 75, 199.
8. B. Halling-Sørensen, G. Sengeløv, J. Tjørnelund. Toxicity of tetracyclines and tetracycline degradation products to environmentally relevant bacteria, including selected tetracycline-resistant bacteria, *Arch. Environ. Contam. Toxicol.* **2002**, 42, 263.
9. A. Mandelbaum. Stereochemical effects in mass spectrometry, *Mass Spectrom. Rev.* **1983**, 2, 223.
10. T. Dai, C. Zhang, Y. Geng, Y. Pan, L. He. A rapid assay of identification for glimepiride and its *cis*-isomer by tandem mass spectrometry, *Talanta* **2018**, 187,

172.

11. D. Wan, H. Yang, C. Yan, F. Song, Z. Liu, S. Liu. Differentiation of glucose-containing disaccharides isomers by fragmentation of the deprotonated non-covalent dimers using negative electrospray ionization tandem mass spectrometry, *Talanta* **2013**, 115, 870.
12. O. Kanie, Y. Shioiri, K. Ogata, W. Uchida, S. Daikoku, K. Suzuki, S. Nakamura, Y. Ito. Diastereomeric resolution directed towards chirality determination focussing on gas-phase energetics of coordinated sodium dissociation, *Sci. Rep.* **2016**, 6, 24005.
13. T. Mochizuki, T. Takayama, K. Todoroki, K. Inoue, J.Z. Min, T. Toyo'oka. Towards the chiral metabolomics: liquid chromatography-mass spectrometry based *DL*-amino acid analysis after labeling with a new chiral reagent, (S)-2,5-dioxopyrrolidin-1-yl-1-(4,6-dimethoxy-1,3,
5-triazin-2-yl)pyrrolidine-2-carboxylate, and the application to saliva of healthy volunteers, *Anal. Chim. Acta.* **2015**, 875, 73.
14. S.A. McLuckey, R.G. Cooks. *Angle- and energy-resolved fragmentation spectra from tandem mass spectrometry*, Wiley, New York, **1983**.
15. M. Šala, D. Kočar, T. Lukežič, G. Kosec, M. Hodošček, H. Petković. Rapid identification of atypical tetracyclines using tandem mass spectrometric fragmentation patterns, *Rapid Commun. Mass Spectrom.* **2015**, 29, 1556.
16. M.J. Frisch, G.W. Trucks, H.B. Schlegel, G.E. Scuseria, M.A. Robb, J.R. Cheeseman, J.A. Montgomery Jr., T. Vreven, K.N. Kudin, J.C. Burant, J.M.

Millam, S.S. Iyengar, J. Tomasi, V. Barone, B. Mennucci, M. Cossi, G. Scalmani, N. Rega, G.A. Petersson, H. Nakatsuji, M. Hada, M. Ehara, K. Toyota, R. Fukuda, J. Hasegawa, M. Ishida, T. Nakajima, Y. Honda, O. Kitao, H. Nakai, M. Klene, X. Li, J.E. Knox, H.P. Hratchian, J.B. Cross, C. Adamo, J. Jaramillo, R. Gomperts, R.E. Stratmann, O. Yazyev, A.J. Austin, R. Cammi, C. Pomelli, J.W. Ochterski, P.Y. Ayala, K. Morokuma, G.A. Voth, P. Salvador, J.J. Dannenberg, V.G. Zakrzewski, S. Dapprich, A.D. Daniels, M.C. Strain, O. Farkas, D.K. Malick, A.D. Rabuck, K. Raghavachari, J.B. Foresman, J.V. Ortiz, Q. Cui, A.G. Baboul, S. Clifford, J. Cioslowski, B.B. Stefanov, G. Liu, A. Liashenko, P. Piskorz, I. Komaromi, R.L. Martin, D.J. Fox, T. Keith, M.A. Al-Laham, C.Y. Peng, A. Nanayakkara, M. Challacombe, P.M.W. Gill, B. Johnson, W. Chen, M.W. Wong, C. Gonzalez, J.A. Pople, Gaussian 03. Gaussian, Inc.: Pittsburgh, PA, **2003**.

17. A.M. Kamel, H.G. Fouda, P.R. Brown, B. Munson. Mass spectral characterization of tetracyclines by electrospray ionization, H/D exchange, and multiple stage mass spectrometry, *J. Am. Soc. Mass Spectrom.* **2002**, 13, 543.
18. G. Ma, G. Liu, S. Shen, Y. Chai, L. Yue, S. Zhao, Y. Pan. Competitive benzyl cation transfer and proton transfer: collision-induced mass spectrometric fragmentation of protonated N,N-dibenzylaniline, *J. Mass Spectrom.* **2017**, 52, 197.
19. A.R. Dongré, J.L. Jones, Á. Somogyi, V.H. Wysocki. Influence of peptide composition, gas-phase basicity, and chemical modification on fragmentation efficiency: evidence for the mobile proton model, *J. Am. Chem. Soc.* **1996**, 35,

8365.

20. L. Yue, J. Li, X. Xie, C. Guo, X. Yin, Q. Yin, Y. Chen, Y. Pan, C. Ding. *Ortho*-hydroxyl effect and proton transfer via ion–neutral complex: the fragmentation study of protonated imine resveratrol analogues in mass spectrometry, *J. Mass Spectrom.* **2016**, 51, 518.

SUPPORTING INFORMATION

Additional supporting information may be found online in the Supporting Information section at the end of the article.

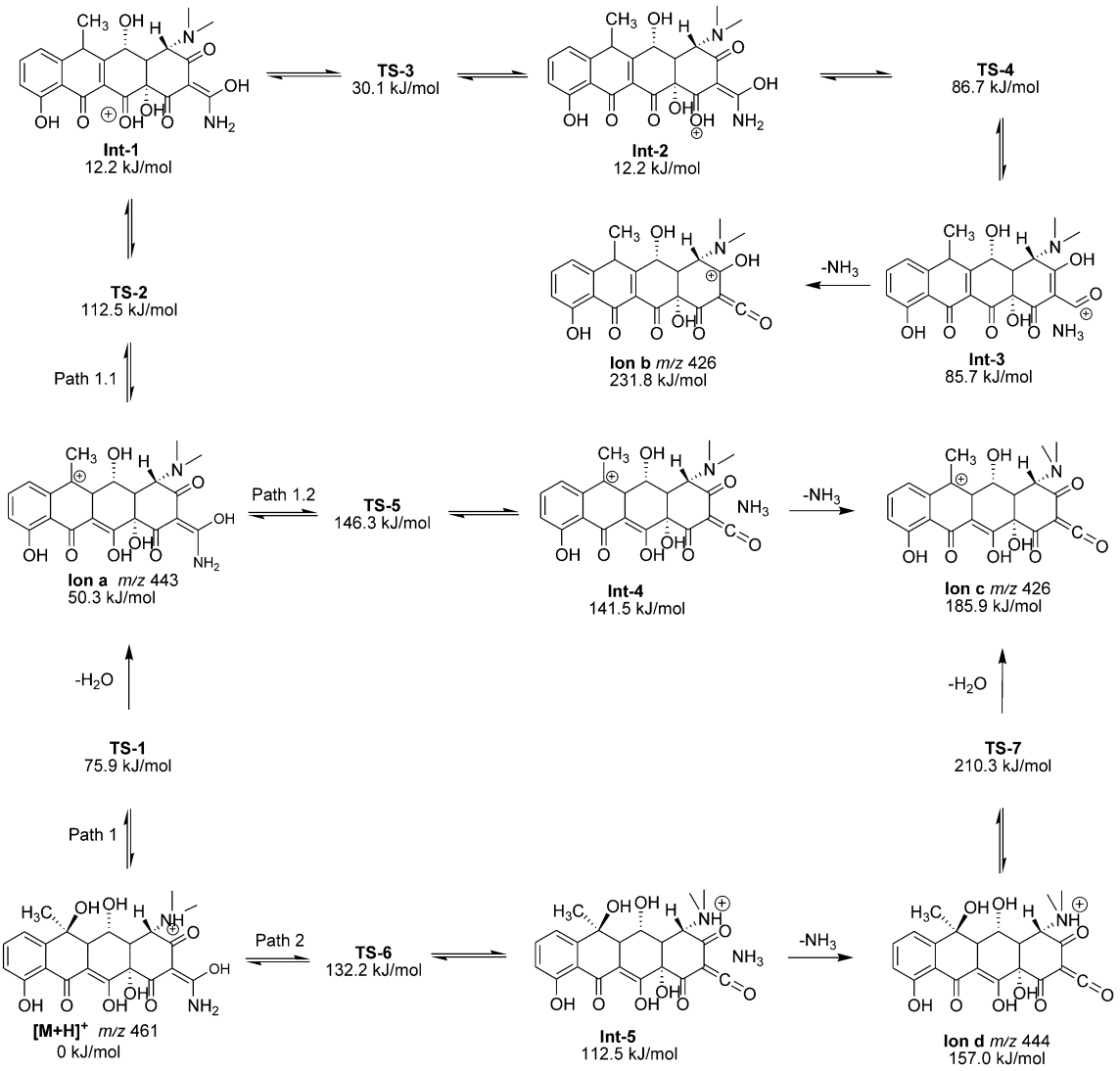

SCHEME 1 Fragmentation pathways of protonated oxytetracycline.

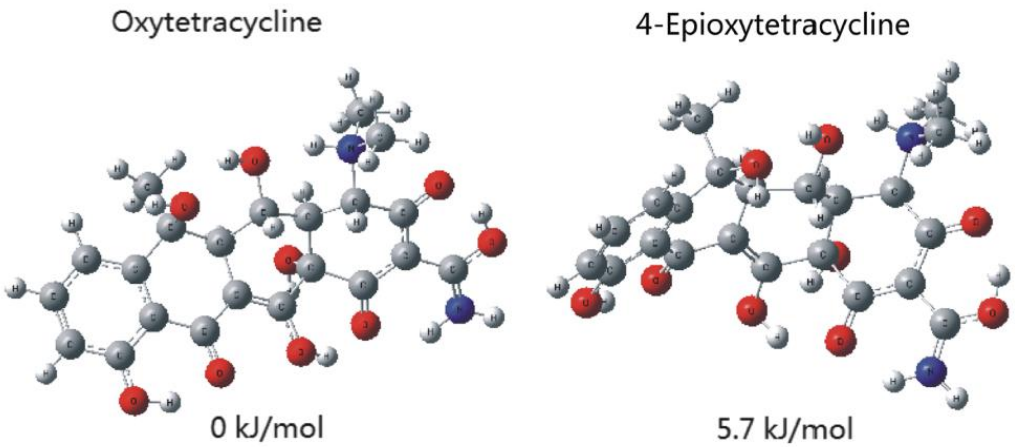

FIGURE 1 Optimized conformation of protonated oxytetracycline and its 4-epimer.

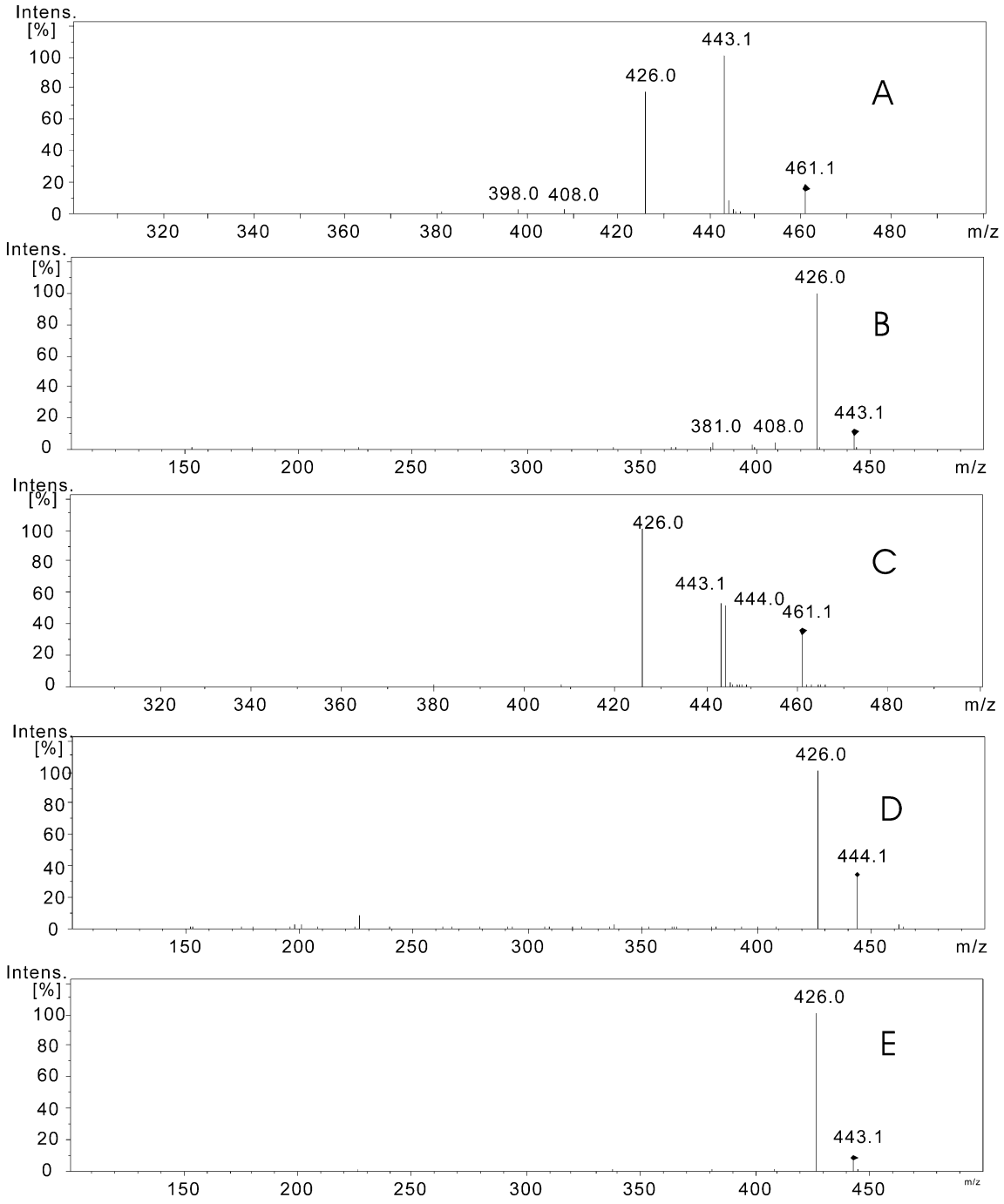

FIGURE 2 CID mass spectrum of (A) protonated oxytetracycline, (B) the ion at *m/z* 443 from protonated oxytetracycline, (C) protonated 4-epioxytetracycline, (D) the ion at *m/z* 444 from protonated 4-epioxytetracycline, (E) the ion at *m/z* 443 from protonated 4-epioxytetracycline.

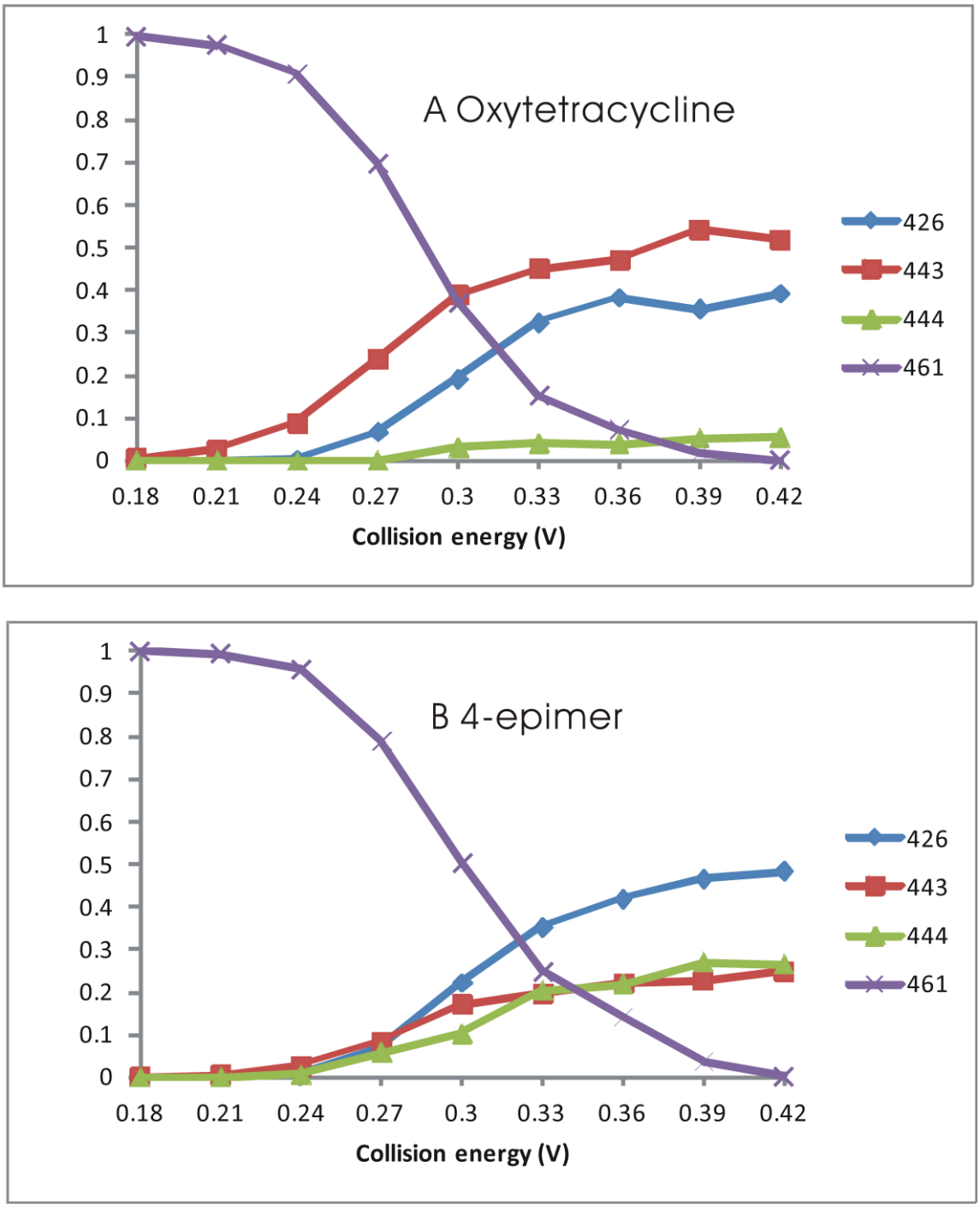

FIGURE 3 Breakdown curves of (A) oxytetracycline and (B) 4-epioxytetracycline.

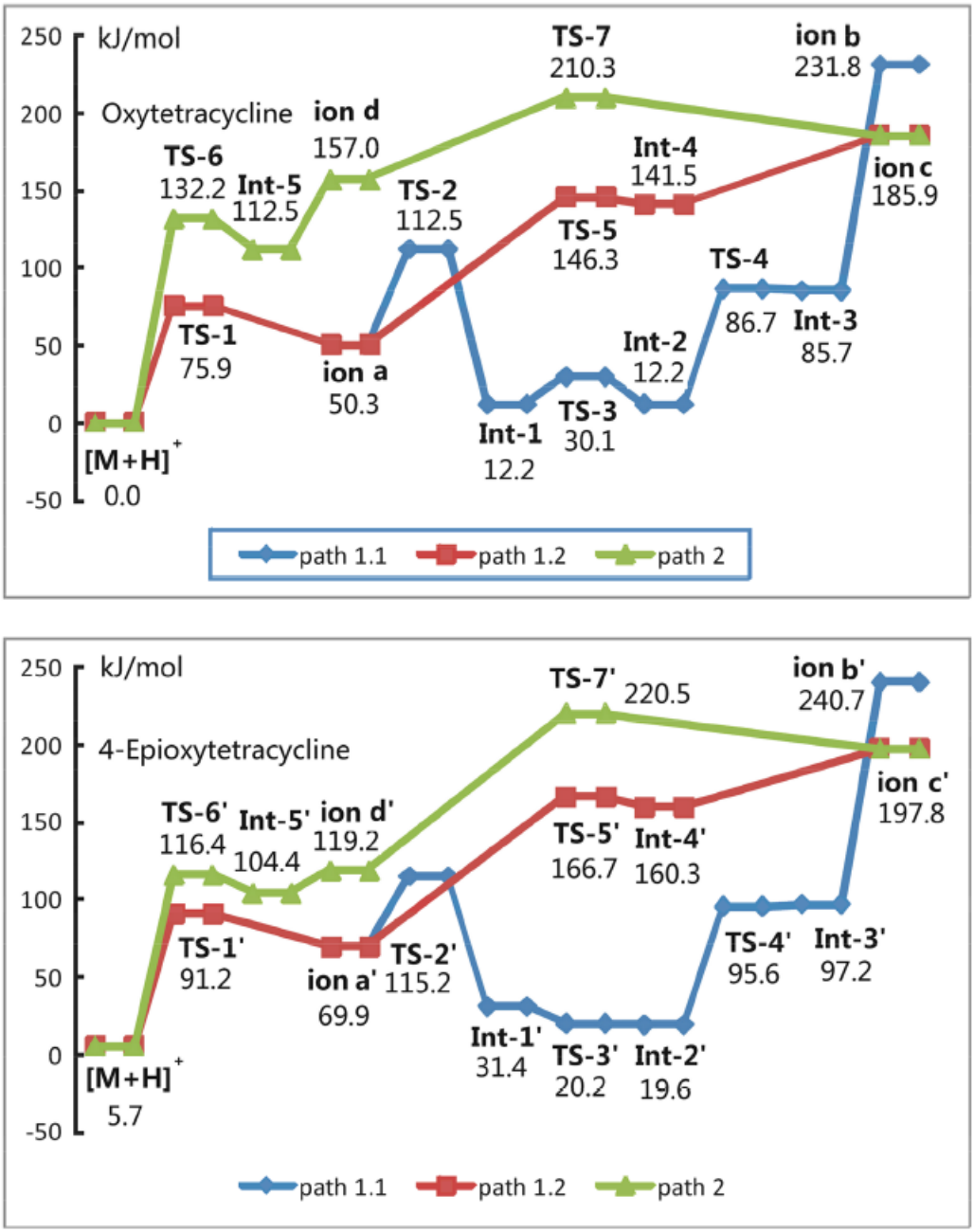

FIGURE 4 Potential energy diagrams for fragmentation of $[M+H]^+$ of oxytetracycline and its 4-epimer following the paths indicated in Scheme 1.